Microarrays for the study of compartmentalized microorganisms in alginate microbeads and (W/O/W) double emulsions

Armend G. Håti[a], Nina Bjørk Arnfinnsdottir[a], Camilla Østevold[a], Marit Sletmoen[b], Gianluca Etienne[c], Esther Amstad[c], Bjørn T. Stokke[a]

Understanding of cells has mainly been achieved through analysis of average properties of large cellular populations. The increased awareness of cellular heterogeneity in various biological systems, spanning from single bacterial cells to human tissue calls for alternative approaches. The need to understand cellular heterogeneity has motivated the development of instrumentation, protocols, and methods for analyzing single cells. In this paper we demonstrate how microorganisms encapsulated in micron sized alginate microbeads with droplet based microfluidcs can be immobilized on microarrays on glass surfaces by virtue of micro contact printing. The microarray presentation opens for efficient microscopic inspection of high numbers of single cells as well as colony picking by selectitive microbead aspiration as demonstrated herein. We also present a double emulsion (W/O/W) micro-array arrangement strategy for the investigation of swimming microorganisms with focus on the widely studied *P.putida*.

Introduction

Isogenic microbial populations often exhibit significant variability in gene expression at the single cell level.[1, 2] Standard approaches for the investigation of microbial populations are still dominated by bulk measurements, which provide data related to the average properties of the population. The awareness of the limitations of these approaches, including lack of ability to clearly resolve statistically rare events and phenotypic variation within microbial populations, has motivated development of new approaches. Recent progress within such approaches aim at cultivation and analysis at the single cell level.[3-6] The proposed approaches also include the positioning of single cells in 2D microarrays thus enabling tracking of the growth and expression level of individual cells.[7-9] The microarray approach enables easier screening including toxicity testing[10] and identification of persister cells in bacterial colonies.[11]

Different strategies have been reported to obtain 2D microarrays of bacterial cells on flat surfaces. Examples of this include the preparation of structured substrates that capture bacteria in physical structures,[12, 13] selective adhesion of bacteria onto regions functionalized with chemicals that promote bacterial adhesion[7, 8, 14] and direct deposition of the bacteria in a predefined pattern by either micro contact printing[15, 16] or droplet deposition.[17-19] The 2D microarray approach based on selective adhesion of single- or only a few bacteria on each functionalized surface spot has some inherent challenges. One of the main hurdles of this approach is the need for chemical patterns with features in the same size range as the microorganisms, which requires equipment allowing deposition of molecules with nano- and micrometer precision (e.g. photo- or electron beam lithography and/or etching). Additionally, the immobilization of microorganisms is based on their specific interaction within the patterned domain as governed by the chemical properties of the imprinted and inert material as well as the surface chemistry of the microorganism. The specific surface chemistry of the microorganisms is thus mechanistic in successful application of the microarray and limits the transferability of a particular adhesive compound on the array to a different organism. This calls for tailoring the selection of the adhesive component, and thus limits the versatility of these microarrays. Moreover, the surface immobilization procedure and the choice of adhesive chemicals in the patterns may affect the microorganism (e.g. viability).[20] Challenges may arise in colony formation studies as the increasing number of daughter cells will gradually either cover the entire microarray surface, or release into solution and thereby render the analysis challenging.

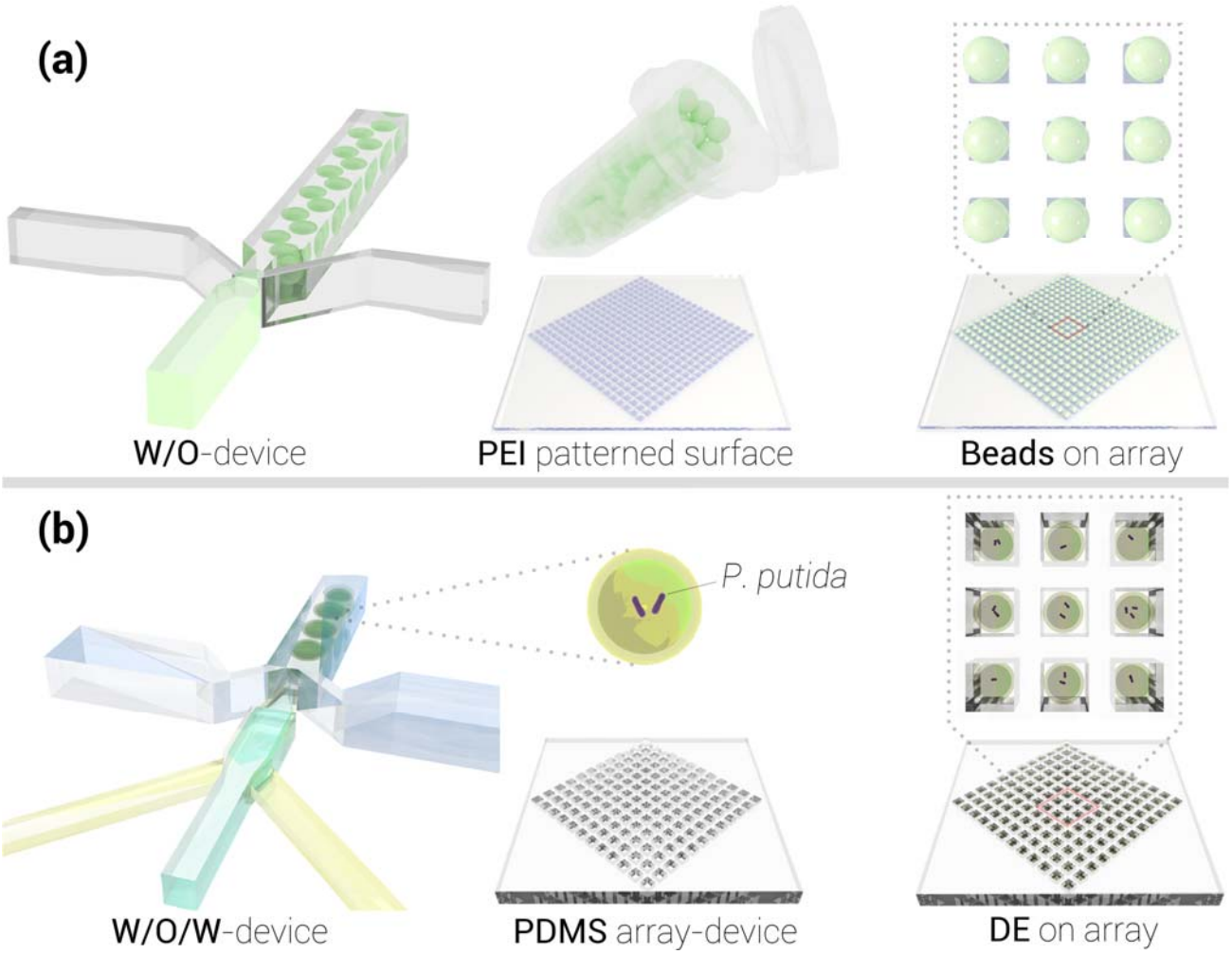

Fig. 1 A schematic of the work-flow presented in this paper. *(a)* Microorganism-laden alginate microbeads were arranged onto PEI patterned microarrays by virtue of droplet based microfluidics and micro contact printing. *(b)* Double emulsions (W/O/W) were also investigated as compartments for *P. putida* and were arranged in microarrays within a 3D PDMS microarray chamber device.

Droplet-based microfluidics has been widely applied to produce monodisperse emulsions of precursor polymer solutions, a process that also can be used to encapsulate cells and subsequent crosslinking of the precursor polymers to form spherical microbeads.[21-23] The porous 3D hydrogel structure represents natural niches for the microorganism and may be applied to support investigation of cellular response to a variety of stimuli and environmental conditions at the single cell level. For example, encapsulated cells may be exposed to drugs and antibiotics for screening through the hydrogel matrix as these structures allow for diffusion of small molecules through the polymeric network. Different polymers, both synthetic and natural, have been used to prepare gels for cell entrapment or encapsulation.[24, 25] Alginate, a linear polysaccharide consisting of β-D-mannuronic (M) and α-L-guluronic (G) acid residues stands out in terms of the polymers biocompatible nature, in addition to allowing gelation under relatively mild conditions to from hydrogels.[23, 26]

Several approaches have shown good control of microbead organization including optically induced dielectrophoresis,[27] nanoplotters to pattern precursor solution of alginate followed by subsequent gelation[10] and microfluidics supported organization of alginate beads in microchannels.[28]

In this paper we demonstrate how microorganisms encapsulated in micron sized alginate hydrogels by virtue of droplet based microfluidics can be anchored to polyethylene imine (PEI) functionalized patterns using microcontact printing (μCP). Unlike the previously proposed direct immobilization of cells onto solid supports,[8, 13, 14] the method does not require specific cell surface properties. The anchoring of the microbeads does not depend on the properties of the microorganism trapped in the gel and relies solely on the interaction between alginate in the microbead and PEI as these polymers are oppositely charged. The proposed approach opens new possibilities for studies of single cells contained in a 3D matrix over prolonged periods of time in a systematic and straightforward manner. Encapsulated and micro-organized bacteria may serve as a protocol that enables investigation of spatial heterogeneity in bacterial biofilms with possibility of integrating the platform with chemical-concentration gradients to evaluate bacterial adaptation to various local chemical environment[29] given the permeability of the alginate hydrogels.

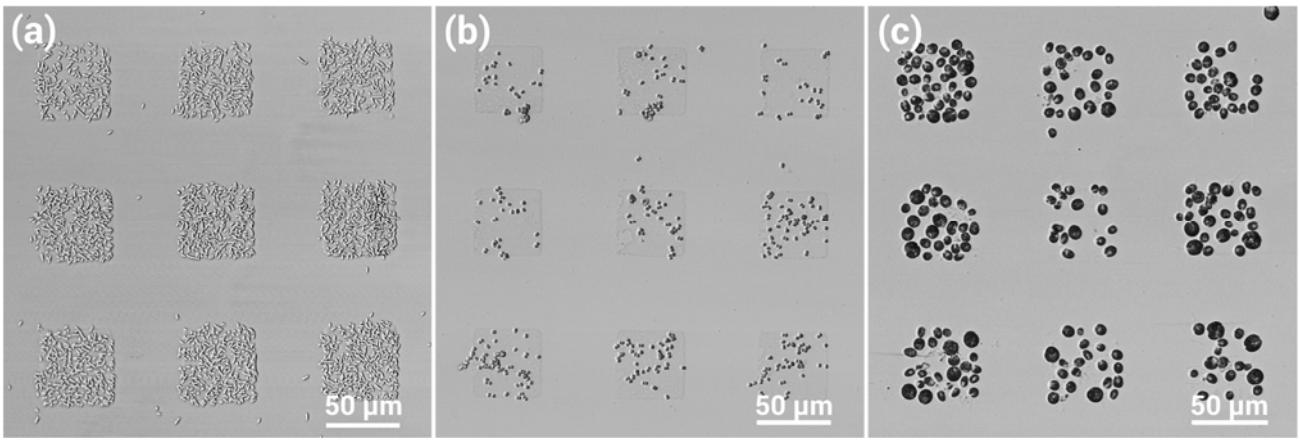

Fig. 2 Optical micrographs of bacteria and algae immobilized on square shaped spots of PEI deposited using µCP on PEGylated glass surfaces; (a): *P. putida* KT2440, (b) *Synechocystis sp.* PCC 6803 and (c): *Chlamydomonas reinhardtii* CC-4532.

We also demonstrate the arrangement of *P. putida*-laden double emulsions (W/O/W) with fluorinated oil shells for the investigation of interactions between swimming microorganisms, which the alginate microbead strategy cannot offer due to constraining the mobility of the microorganisms upon gelation of the microbeads. Such structures have recently gained much attention for the compartmentalization of cells as the fluorinated oil shell enables transport of small molecules across and have demonstrated high oxygen transport.[30, 31] The presented strategy will potentially enable investigation of important single-bacterial events, such as plasmid transfer via conjugation, which is of paramount importance as we find ourselves in a time with a growing issue of spread of antibiotic resistance in bacteria.[32, 33]

Results and discussion

2D-arrangement of microorganisms

Three widely explored microorganisms; the bacterium *P. putida* K2440, the cyanobacterium *Synechocystis sp.* PCC 6803 and the algae *Chlamydomonas reinhardtii* CC-4532 were investigated and were all successfully immobilized onto pre-defined 50 µm square shaped PEI coated spots on PEGylated glass surfaces (Fig. 2). The number of bacteria anchored per spot, varied among the different microorganisms, and *P. putida* were found to have the highest surface coverage of the PEI spots. Microorganisms immobilized onto surfaces allow single cell studies under controlled environmental conditions. Characterization at the single cell level of microorganisms immobilized by this strategy can be can be conducted by image analysis software capable of recognizing and temporal monitoring of single bacteria in larger colonies or by optimization of the pattered features in order to facilitate arrays of single bacteria. If incorporating the surfaces into a microfluidic cultivation system, fresh medium can be continuously added without removing the cells. This is an important advantage compared to the agar pads traditionally used in studies of colony formation. However, despite the successful immobilization of the microorganisms directly onto the PEI patterns, immobilization via this route is limited in terms of variable attachment density. For single cell arrays there is also an added technical challenge in fabricating patterns with features on the scale of only a few µm. In addition, it has been shown that nonadherent cell types, including cell lines adapted for industrial fermentation in suspension, present unique challenges for microfluidic analysis due to the required immobilization during medium exchange.[5] Furthermore, immobilization of microorgansims on 2D microarray does not allow for extensive studies of microorganism proliferation as the microorganisms do not sticking firmly together are prone to escape the patterns upon colony expansion. This ultimately hampers reliable studies of cell growth over many generations. This is a significant drawback since growth is recognized as one of the most important performance indicators in biotechnological production processes.[4] Furthermore, PEI is potentially detrimental to the microorganism and has previously been shown to have cytotoxic effects on fibroblasts and osteoblasts ,[34] even though the molecule is applied to mediated DNA transfection.[35]

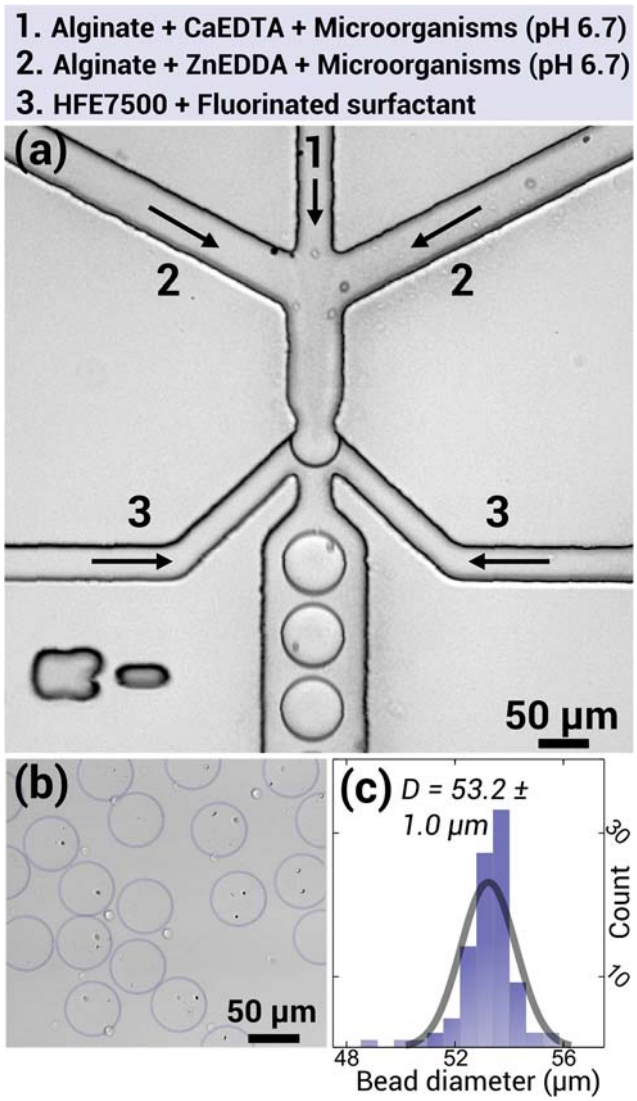

Fig. 3 A droplet-based microfluidic device was utilized for the facile encapsulation of microorganisms and subsequent gelation to form cell-laden alginate microbeads. *(a)* Micrograph of the droplet based microfluidic device in the region at which droplet breakup occurs due to the incoming fluorinated oil containing fluorosurfactant. Two aqueous precursor alginate flows are necessary to allow for gelling of the droplets using a gelling method that relies on an ionic exchange mechanism recently developed by our group. *(b)* Micrograph of collected alginate hydrogels in TAP medium, in this case loaded with Synechocystis sp. PCC 6803. *(c)* Experimentally determined size distribution of the alginate hydrogels (histogram) and fit of Gaussian to estimate mean diameter. The diameter of the individual beads was determined using image analysis carried out using MATLAB (MathWorks®) of micrographs as the one in *(b)*.

3D-arranged microorganism-laden alginate beads

In order to overcome the inherent limitations of 2D immobilization of microorganisms on PEI micro patterns we explored microfluidics aided encapsulation of the microorganisms in biocompatible alginate microbeads. Fig. 3 presents the microfluidic based procedure used for encapsulation of microorganism in alginate beads. The device supports production of monodisperse droplets consisting of precursor alginate solutions and microorganisms that are gelled down-stream towards the outlet of the microfluidic device. The aqueous alginate polymers are ionically crosslinked exploiting a competitive ion exchange crosslinking (CLEX) mechanism for internal gelation of the alginate under mild conditions and at physiological pH (pH = 6.7).[36, 37] In short, two aqueous alginate precursor solutions; one containing CaEDTA and the other containing ZnEDDA meet in a microfluidic channel prior to droplet-breakup (Fig. 3a), whereby mixing of the two solutions facilitates binding of Zn^{2+} to EDTA, rendering Ca^{2+} free to crosslink alginate to form a hydrogel. The gelation method is carried out under constant pH and temperature and excellent cell viability has previously been demonstrated with this method.[36, 37] The population of microbeads obtained using this approach was nearly monodisperse (Fig. 3b) with an estimated diameter of 53.2 ± 1.0 µm (Fig. 3c). The image in Fig. 3c depicts encapsulated *Synechocystis sp.* and such images were analysed to calculate the average bead diameter.

The preparation of alginate hydrogels in the flow-focusing microfluidic device did not yield gelation in the stagnation point in the microfluidic channels, even after 12 hours of continuous microbead synthesis in the same device. The density of microorganisms contained in the alginate gel is determined by the concentration of the cells in the alginate solutions, and the number of microorganisms in each bead has been shown to follow a Poisson distribution. Encapsulation of only single microorganisms in each bead therefore require alternative approaches.[38]

The alginate microbeads adhered readily to the PEI spotted areas with only a few vacancies upon addition of microorganism-laden beads. The approach thus provides a simple and efficient route for anchoring of alginate microbeads loaded with microorganisms on the PEI patterns (Fig. 4) and is not dependent on the specific adhesion capacity of the adhering chemical pattern and the microorganism. The nature of interaction forces between the alginate gel beads and PEI spots can be expected to have similar molecular mechanisms as those involved in the polyelectrolyte multilayer formation and complexation where increased entropy associated with counterion release in the counterion exchange process is a major contribution.[39, 40] The encapsulated microorganisms displayed high viability and proliferation at doubling times similar to when free in appropriate medium under ideal light and temperature conditions (~24 hours for *Chlamydomonas* and *Synechocystis* [41, 42] and ~1 hour for *P. putida*[43]).

Due to the relatively long doubling time of the *Chlamydomonas* and *Synechocystis* the microarrays of alginate microbeads containing these microorganisms where imaged at 24 hour intervals and kept at constant illumination and with slight agitation between imaging to ensure optimal culturing conditions. The fluorescence from the microorganisms is due to the photosynthetic properties and served as an indication of cell viability during colony growth of the microorganisms within the microbeads. The microorganisms eventually escaped the microbead confinements enabling motility in the surrounding medium. Evidence of such an escape is shown in Fig. 4 where the *Chlamydomonas* colony indicated by a red arrow grew beyond the microbead confinement.

The *P. putida* KT2440 investigated in this study was transfected with coding for Green Fluorescent Protein (GFP) induced by addition of arabinose.[44] Medium with arabinose (50mM) was added to the microbead encapsulated *P. putida* KT2440 after immobilization onto the PEI patterns. Imaging of the microarray every four hours allowed following *P.putida* colony growth. The emission of fluorescence from the immobilized bacteria was apparent and increased after addition of arabinose as a result of GFP production (Fig. 4). The emission of fluorescent light reflects the expression of GFP, and thus proves efficient delivery of arabinose to the bacteria through the porous alginate hydrogel network. Although diffusion of macromolecules in hydrogels in general can be affected by the network mesh size,[45] this facet appears not to represent a significant rate limiting process in the present case since we observe fluorescence due to GFP production in the bacteria shortly after addition of the initiator. This underlines the versatility of porous hydrogels as 3D confinements for microorganisms since small molecules, e.g. drug molecules or antibiotics, are able to diffuse through the gel network.[25]

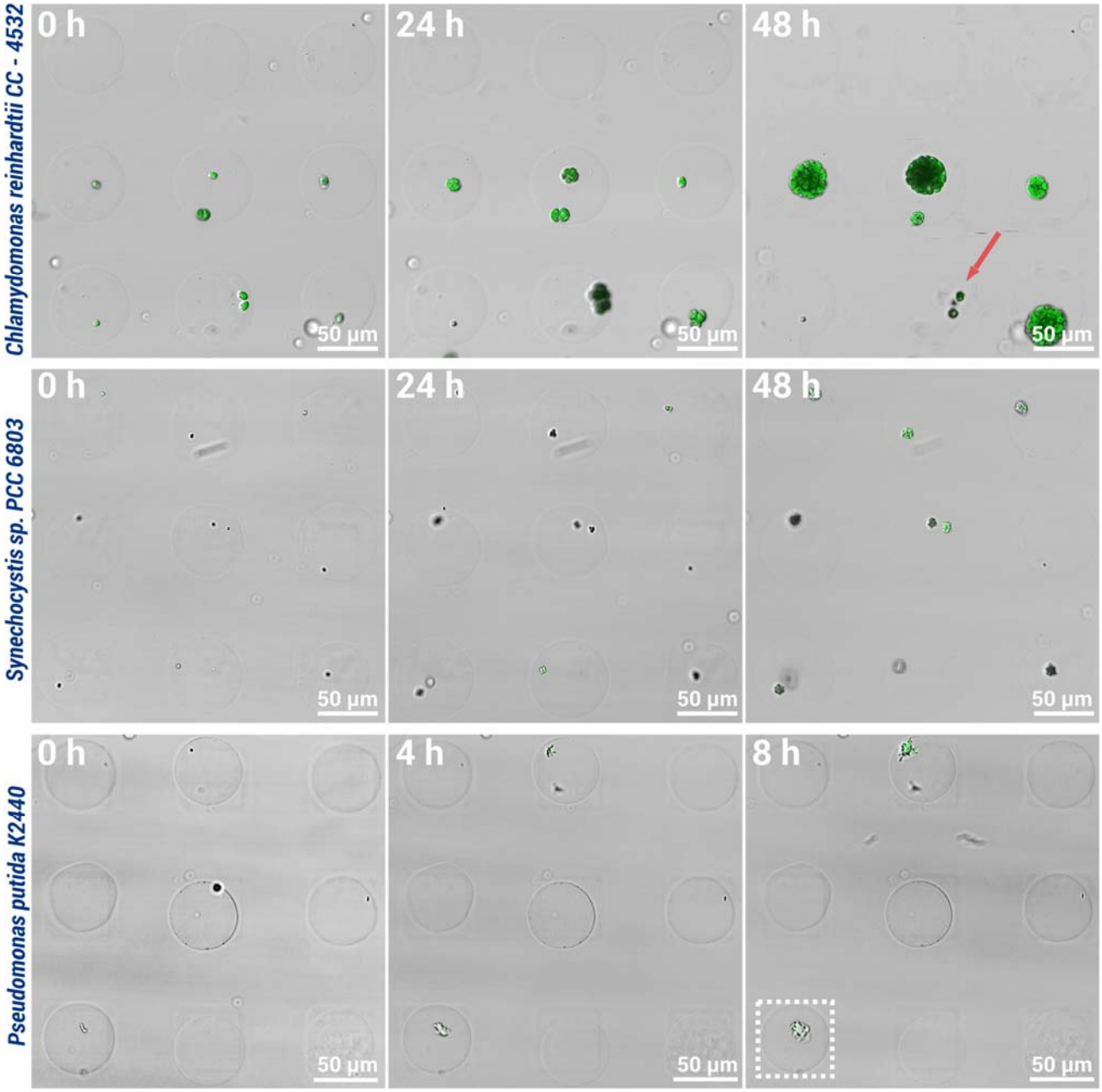

Fig. 4 Micrograph time series of 3x3 alginate microgels immobilized on PEI patterns. The microgels are loaded with *Chlamydomonas reinhardtii* CC-4532 (top row), *Synechocystis sp.* PCC 6803 (middle row) and *P. putida* KT2440 (bottom row) and covered in TAP, BG11 and 10% (v/v) LB in TAP growth medium respectively to maintain growth of the encapsulated microorganisms. The microarrays of encapsulated microorganisms where followed over time to monitor the growth of the cells inside the microgels. All images are merged images of bright field image and fluorescent signal (fluorescent signal from chlorophyll in *Synechosystis* and *Chlamydomonas*, and from induced GFP via addition of arabinose in *P. putida* KT2440) captured with a Leica SP5.

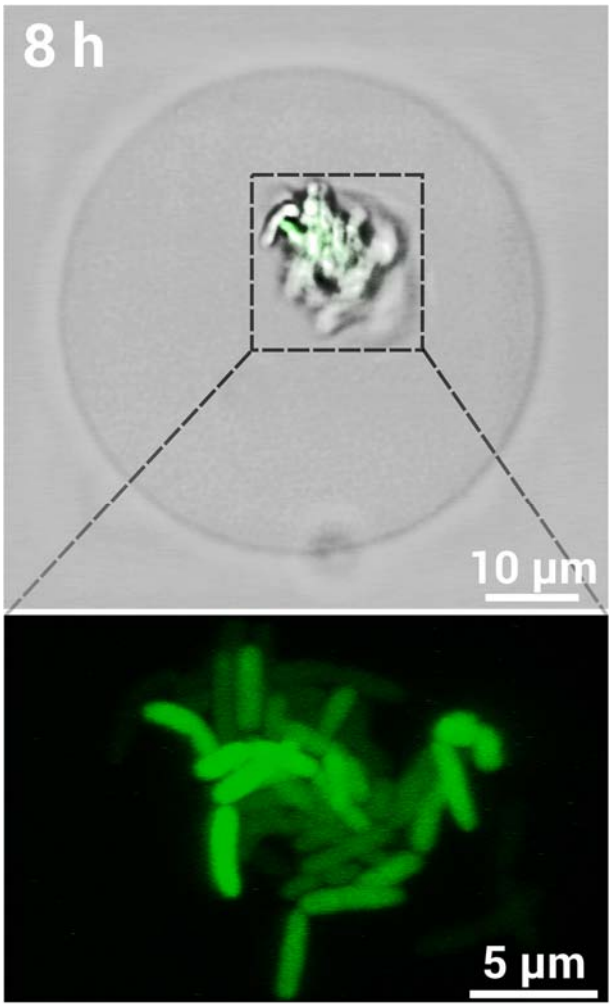

Fig. 5 Top: Image of *P. putida* encapsulated in an alginate microgel immobilized on a PEI pattern (white box in Fig. 4). The image shows the expression of GFP (green) in the bacteria as a result of the added inducer reflecting ability of the arabinose to diffuse through the alginate hydrogel. The image is a merged image of bright field and fluorescent channels. Bottom: A 3D projection of a z-stack of images of the fluorescence signal from GFP expressed by the bacteria. The image shows the 3D structure of the bacterial colony inside the bead. Imaged with a Leica SP5.

Furthermore, a 3D-projection of a *P.putida* colony within the microbeads displays the 3D nature of the colony growth in contrast to the growth of bacteria on 2D surfaces such as cell flasks or PEI patterns (Fig. 5, ESI Video 1). As previously shown[4] all 3D and 2D systems share the difficulty of reliable identification and tracking of individual cells, especially in densely packed microcolonies. These challenges can to some extent be overcome by sophisticated image recognition software.

Aspiration and re-suspension of selected encapsulated bacteria

The arrays of cell-loaded microbeads presented here could also be envisioned as a screening platform for simple detection and isolation of cells of special interest based on expression of fluorescent signals. To demonstrate this, we encapsulated a mixture of two strains of *P. putida* KT2440; one carrying the pSB-B1 plasmid and one carrying the pHH100-GFP plasmid. The bacteria carrying the pSB-B1 plasmid could thus easily be identified by their expression of GFP after addition of arabinose to the culture medium (Fig. 6a). A micromanipulator was utilized to position a micropipette for capturing and transferring a single microbead with a particular fluorescent bacterium (Fig. 6b). This microbead was subsequently placed in culture medium and incubated overnight resulting in a growth of bacteria that expressed GFP upon induction with arabinose (Fig. 6c). We thus demonstrated that selective capturing and relocation of single microbeads based on fluorescence from encapsulated cells for further investigation is possible. The proposed encapsulation, micro-organization and subsequent aspiration approach may be implemented to further investigate phenotypic differentiation such as bacterial persistence.[46]

Encapsulation of microorganisms in alginate microbeads and subsequent organization of these onto microarray patterns supports combining 3D culturing with microscopy based array inspection and microscopy guided colony picking. This strategy is attractive due to the following facets: *(1)* anchoring of encapsulated microcolonies is dependent on hydrogel-micro pattern interactions and thus circumvents the need for selection of microorganism specific adhesive chemistry; *(2)* there is no direct contact between the microorganism and adhesive chemical thus reducing potential

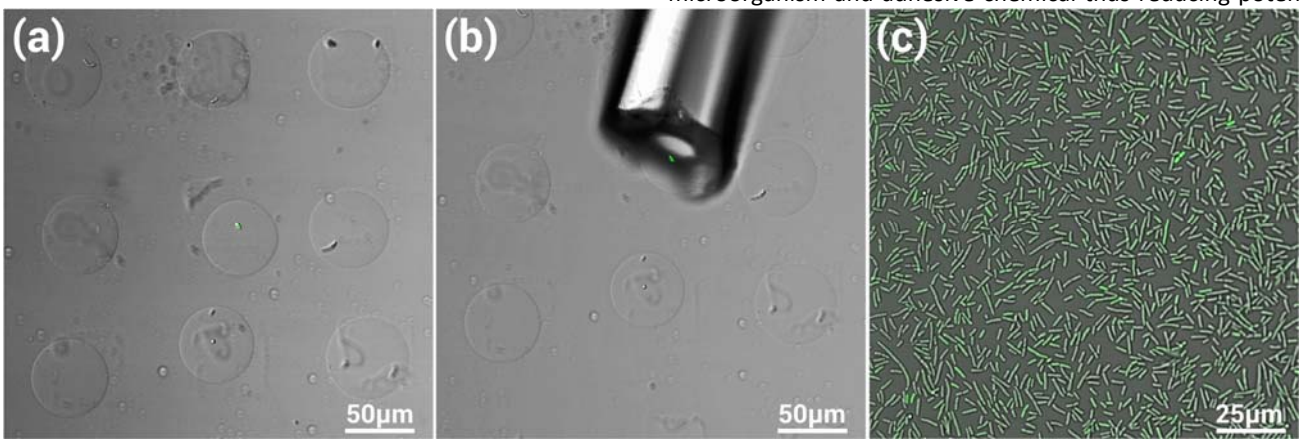

Fig. 6 Micrograph of 3x3 *P.putida* loaded alginate microbeads, similar to the one displayed in Figure 4. 20% of the P.putida population contained the pSB-B1 plasmid and produced GFP upon addition of 50mM arabinose *(b)* A glass capillary mounted on a micro manipulator was utilized to selectively collect one microbead containing *P.putida* with the pSB-B1 plasmid as evident from the fluorescence. *(c)* The collected microbead-encapsulated bacteria were re-suspended in LB medium over-night and imaged after 24h. One hour prior to imaging, the production of GFP by the pSB-B1 plasmid was induced by addition of arabinose (50 mM) in the culture medium. The image is a merged image of bright field and fluorescent channels.

adverse effects associated with its direct contact; *(3)* the microbeads act as a confinement for colony growth; *(4)* free swimming daughter cells can be removed; *(5)* individual microbeads can be manipulated; and *(6)* if, by sorting before anchoring, the beads contains single microorganisms, this can serve as a platform for identifying single cells of interest before the removal of the microbead and further investigations of the microorganism. For instance, a population of cells who all are the descendants of the same mother cell can be obtained by incubation of the microbead.

3D-arranged *P. putida*-laden double emulsions

Constraining mobility of swimming microorganisms in 3D alginate microbeads, such as the *P. putida* and the *Chlamydomonas* studied herein will drastically lower the chances of direct cell-cell interactions since the microorganisms will be at arbitrary locations within the single emulsion at the point of gelation. Water-in-oil single emulsions alone have several limitations that restrict their application as microcapsules for living materials. The oil carrier fluid does not allow continuous supply of nutrient or inducer molecules, and is incompatible with aqueous phase-based analysis such as flow cytometry,[30, 47, 48] for example. Therefore, double emulsions (W/O/W) with fluorinated oil shells (HFE7500, 3M®) were investigated as compartments for *P. putida*. Double emulsions are preferred over single emulsions, particularly due to demonstrated transport of small molecules both in and out of the capsule via the semi-permeable oil layer.[30] Fluorinated oil also enable transport of oxygen to maintain a healthy environment for the microorganisms.[49]

A recently proposed droplet-based microfluidic device was utilized for the one-step facile production of double emulsions (Fig. 7a).[50] The 3D geometries allow for straightforward hydrophilic and fluorophilic surface treatment, which is a prerequisite for effective production of double emulsions in microfluidic devices.[51, 52] *P. putida* KT2440 carrying the pHH100-GFP plasmid were successfully encapsulated in the double emulsion cores (Fig. 7b), which consisted of low concentration of alginate (0.15% wt/vol) in LB-growth medium. The addition of alginate was necessary to increase the viscosity of the inner aqueous phase and allow for a steady co-flow between this fluid and the fluorinated oil with 1% (wt/vol) fluorinated surfactant (Fig. 7a). The osmotic pressure between the inner and outer aqueous phase was balanced by addition of sucrose (100 g L^{-1}) in the polyvinyl alcohol (PVA, 10% wt/vol) and LB-containing outer aqueous phase. Use of PVA facilitates droplet break-up by increasing the outer aqueous phase viscosity and it functions as a surfactant. Using flow rates of 50 µL h^{-1}, 200 µL h^{-1} and 800 µL h^{-1}, for the inner, middle and outer phase, respectively, resulted in double emulsions with inner diameter of 44.4 ± 2.4 µm and outer diameter of 76.1 ± 1.7 µm (Fig. 7c).

P. putida-laden double emulsions were arranged in microarrays inside a 3D PDMS-based microarray chamber (Fig. 8). Injection of *P. putida*-laden double emulsions in the microarray chamber device was straightforward (ESI Fig.1) and no surface treatment of this device was needed. The microarray consists of an overlaid microchannel (80 µm tall) on arrays of 90 µm x 90 µm x 80 µm wells (xyz) and the larger density of the fluorinated oil shell (1614 kg m^{-3} at 25°C) compared to the surrounding medium enabled sedimentation of one double emulsion per microwell. After sedimentation and systematic arrangement of the *P.putida*-laden double emulsions, an LB-containing aqueous phase with 10% (wt/vol) PVA and 0.5 mM m-Toluic acid was used to flush out free double emulsions and initiate GFP production in the encapsulated *P. putida.* GFP production was indeed detected based on fluorescent signal from the bacteria (Fig. 8), which confirms the transport of m-Toluic acid across the fluorinated oil shell. The systematically arranged double emulsions with encapsulated *P. putida* were simple to locate and monitor over longer time spans with a confocal microscope and swimming *P. putida* inside the double emulsion cores were indeed observed (ESI Video 2). Double emulsion encapsulated *P. putida* displayed high viability and proliferation as can be seen in the time-series micrographs in Fig. 8. After 4 hours, some of

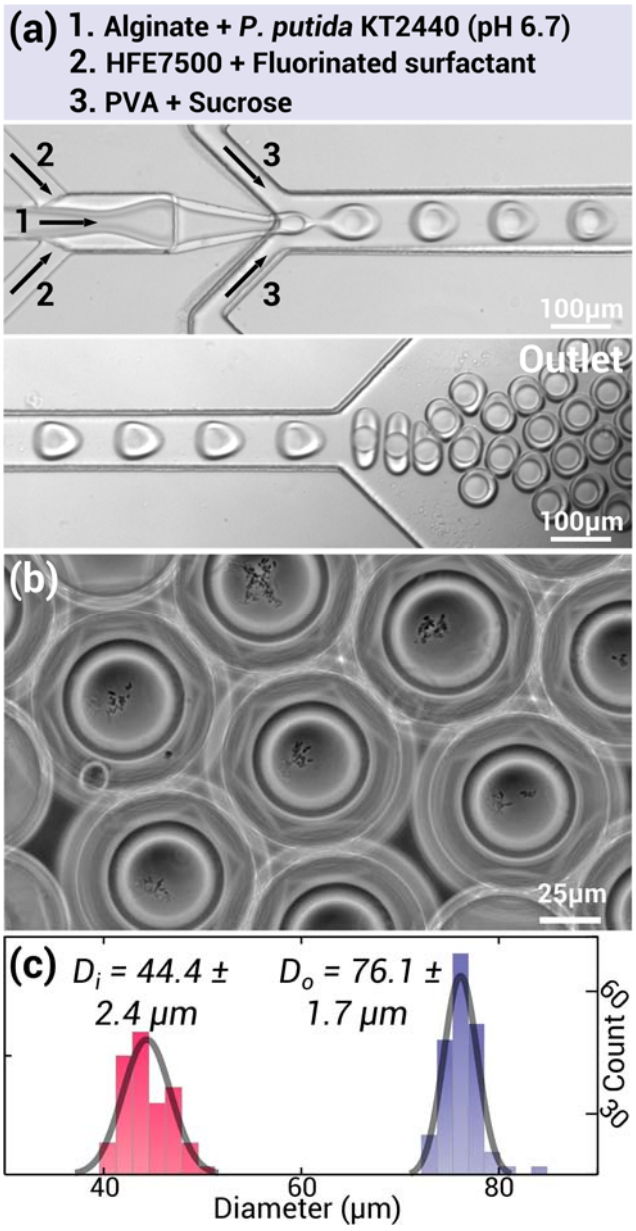

Fig. 7 *(a) P. putida* KT2440 were encapsulated in double emulsions utilizing a 3D droplet based microfluidic device. *(b)* A phase contrast image of *P. putida*-laden double emulsions captured with a quantitative phase contrast microscope (Zeiss axio observer Z1). *(c)* The produced double emulsions displayed a narrow size distribution for both the inner core size (D_i) and outer dimension (D_o).

the double emulsions burst (red arrows, Fig. 8), which is presumably attributed to minor differences in the osmotic pressure between the inner and outer aqueous phase.

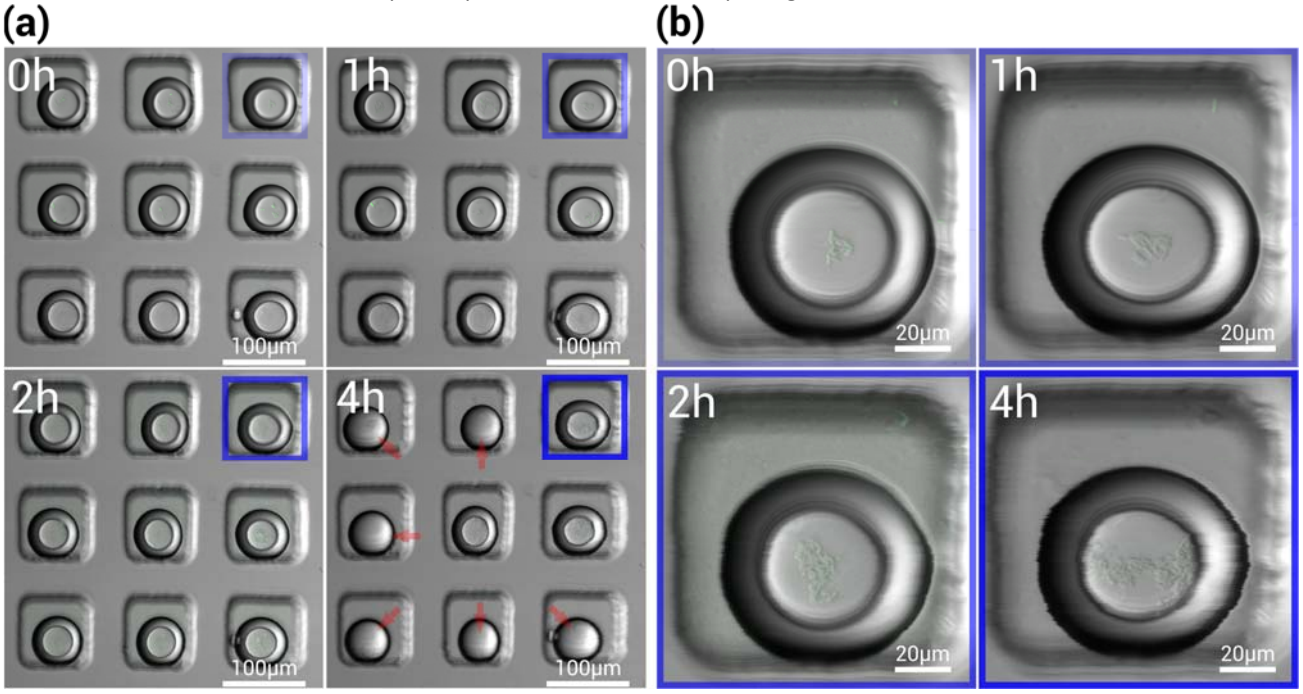

Fig. 8 *(a)* Micrograph time series of 3x3 double emulsions in a 3D PDMS microarray device. The double emulsions are laden with *P. putida* and covered in LB medium containing 10% (wt/vol) PVA, sucrose (100 g L^{-1}) and m-Toluic acid (0.5 mM). The microarrays of encapsulated *P. putida* where followed over 4 hours to monitor the growth of the cells inside the double emulsions. The fluorescence signal from the *P. putida* indicates GFP production as a consequence of transport of m-Toluic acid across the double emulsion layer. Some of the double emulsions burst after 4 hours indicating an imbalance of osmotic pressure between the core and surrounding of the double emulsions *(b)* Magnification of the boxed areas (blue) in *(a)*. All images are merged images of bright field image and fluorescent signal captured with a confocal microscope (Leica SP5).

Finally, we demonstrate the use of CLEX to gel double emulsion cores containing alginate with a modified (4-inlet) design of the original design suggested by Arriaga and co-workers (ESI Fig. 2).[50] In this device, two alginate solutions, one containing 36 mM CaEDTA and the other containing 36 mM ZnEDDA, both with 36 mM MOPS and a final pH of 6.7, were injected via separate inlets and meet in a co-flow region in the device (ESI Fig. 2a). A higher concentration of alginate was necessary to enable gelation of the core. We use 0.6% (wt/vol) alginate instead of 0.15% (wt/vol) as was previously used for the encapsulation of *P. putida* in double emulsions. The device was operated for over 6 hours and no stagnation point gelation was observed, even though the two alginate streams are in contact for ~0.2 seconds prior to double emulsion formation (net flow rate of 100 µL h^{-1} through a 5000 µm x 50 µm x 20 µm (xyz) microchannel).

Double emulsions with hydrogel cores have recently gained much attention since they may be used as templates for hydrogel-core polymersome synthesis. Hydrogel-core polymersomes offer enhanced stability and sustained release of encapsulated cargo[53] and brings us one step closer to synthesizing artificial cells.[54] While others have opted to produce double-cored double emulsions with one core of $CaCl_2$ and the other of alginate to initiate core-gelation upon coalescence of the two inner emulsions,[55] CLEX gelation is not dependent on producing such structures as the two streams of alginate with chelated gelling and exchange ions may co-flow for relatively long timeframes prior to droplet formation and subsequent gelation of the double emulsion cores.

Experimental

Preparation of precursor solutions

All chemicals were purchased from Sigma-Aldrich unless stated otherwise. Deionized water (DIW) with a resistivity of 15 MΩ cm (Milli-Q™, Millipore) was used for the preparation of all samples. Alginate from *L. hyperborea* stipe with M_W of 275 x 10^3 g mol^{-1} and guluronic-residue fraction of F_G = 0.68 was dissolved in DIW to 3% (wt/vol) and used as stock solution. Two alginate solutions containing *(1)* CaEDTA and MOPS and *(2)* ZnEDDA and MOPS were used to synthesize the alginate microbeads and prepared as follows: *(1)* 0.5 M solution of $CaCl_2$ was mixed with 0.5 M thylenediaminetetraacetic acid (EDTA) and 0.5 M 3-(*N*-morpholino)propanesulfonic acid (MOPS) followed by a pH adjustment to pH 6.7 with HCl and NaOH. 3% (wt/vol) Alginate solution was added to provide a final concentration of 0.6% (wt/vol) alginate, 84 mM Ca^{2+}, 84 mM EDTA, 40 mM MOPS. *(2)* 0.5 M solution of $Zn(CH_3CO_2)_2$ was mixed with ethylenediamine-N,N'-diacetic acid (EDDA) and 0.5 M 3-(*N*-morpholino)propanesulfonic acid (MOPS) followed by a pH adjustment to pH 6.7 with HCl and NaOH. 3% (wt/vol) Alginate solution was added to provide a final concentration of 0.6% (wt/vol) alginate, 84mM Ca^{2+}, 84 mM EDTA, 40 mM MOPS.

The outer aqueous phase used for double emulsion synthesis consisted of 10% (wt/vol) polyvinyl alcohol (PVA, M_W = 13000-23000 g mol^{-1}) and 100 g L^{-1} sucrose. For the inner phase, we used 0.15% (wt/vol) alginate dissolved in Lysogeny broth (LB) growth medium.

For double emulsions synthesis with alginate hydrogel cores, two alginate solutions were used and these were identical to the solutions used to produce alginate microbeads.

Fabrication of microfluidic devices

The microfluidic devices were fabricated using soft-lithography techniques. A negative photoresist (SU8-3050, MicroChem Corp.) was spun onto a silicon wafer (University Wafers) to obtain the desired thickness of the microfluidic device (40 µm). The wafer was subsequently soft baked (65°C for 1 min followed by 95°C for 15 min). Emulsion films were aligned with the CAD designs (JD Photo-Tools, UK) of the microfluidic channels on top of the photoresist coated wafer and exposed with UV light (wavelength 360 nm, exposure energy of 250 mJ/cm^2) to cure the channel features onto the wafer. The wafer was post exposure baked using a hot plate (65°C for 1 min and 95°C for 5 min) and subsequently developed for 8 min while stirring using a resist developer (mr-Dev 600,Micro Resist Technology GmbH, Germany). The wafers were then treated with fluorosilane (1*H*,1*H*,2*H*,2*H*-perfluorooctyl(trichlorosilane)) for 45 min in a vacuum chamber to avoid adhesion of polydimethyl siloxane (PDMS, Dow Corning®). PDMS with 10 wt% initiator (Sylgard 184 kit, Dow Corning®) was casted onto the silanized wafer in a petri dish and baked for 3 hours. The PDMS was subsequently peeled off the SU8 structured wafer, punched with 1 mm diameters to enable connection of plastic tubes at the inlets and outlets, plasma treated using a plasma cleaner (Femto, Diener Electronics) and bonded to a slab of PDMS. The PDMS microfluidic devices were baked for 24h after bonding and treated with 1% (v/v) of fluorosilane stated above in hydrofluoroether (HFE7500, 3M®) for 5 min to make the microfluidic channel surfaces fluorophillic.

The 3D PDMS double emulsion device was fabricated as demonstrated by Arriaga and co-workers (Fig. 7a).[50] In short, the photoresist molds were fabricated as described above with three repeated photolithographic steps to produce structures with three different heights (20 µm, 40 µm and 60 µm). Complementary molds on the same wafer (mirror images) were also made; these having two different heights (20 µm, 40 µm). PDMS was cured on both molds, peeled and punched as described and finally plasma treated and aligned as demonstrated elsewhere.[56] The channel in which the outer aqueous phase enters was rendered hydrophilic by continuous injection of poly(diallyldimethylammonium chloride) solution (Mw = 200 000 - 350 000 g mol^{-1}) dissolved in 2 M NaCl, while simultaneously injecting 1% (v/v) fluorosilane containing HFE7500 from the middle phase channel inlet to render this channel fluorophilic and avoid backflow of the polyelectrolyte. After 5 min, the fluorosilane containing HFE7500 was swapped with pure HF7500 and continuous injection of this liquid was performed until the hydrophilic treatment was completed.

Two complementary molds were made on the same wafer for the fabrication of 3D PDMS microarray chamber devices; one mold for the channel (80 µm tall) and another for the wells (80 µm deep). PDMS was cured on both molds, peeled and punched as described and finally plasma treated and bonded. Alignment of the complementary PDMS parts was aided by the addition of water to delay the bonding process. The water was subsequently removed by heating the device at 65°C for 30 min. The final device is depicted in ESI Fig. 1. No surface treatment was needed for these channels.

Fabrication of PEI microarrays

Microcontact printing (µCP) was used to deposit chemicals in pre-defined patterns on 35mm glass slides from Wilco-dish sets (Wilco Wells). The glass slides were immersed in acetone (VWR), rinsed with 96% ethanol, rinsed with MilliQ water and blow dried with nitrogen prior to the following steps. For PEGylation, the slides were coated with poly-L-lysine (20 000 g mol^{-1}) grafted with PEG (2000 g mol^{-1}) (PLL-g-PEG, Susos) by immersion in aqueous 0.1mg/mL PLL-g-PEG buffered (10 mM HEPES, pH 7.4) solution for 60 minutes. The slides were subsequently rinsed, first in phosphate buffered saline, then in MilliQ water and finally dried with nitrogen. µCP of patterns onto the PEGylated slides was carried out using PDMS stamps as previously reported. [8] PDMS stamps were made using soft lithography, similar to that used for the fabrication of the microfluidic devices. The PDMS stamps were 20 µm tall and consisted of 10 x 10 microarrays of squares (50 x 50 µm) separated by 50 µm and were used to introduce patterns of poly (ethyleneimine) (PEI, Mw 750.000 by LS, 50 wt % in H_2O). The stamps were incubated with aqueous 1 wt% PEI for 15 minutes, blow dried with nitrogen and placed pattern-side down on the PEGylated glass slides for 20 minutes. A weight of 100g was placed on top of the stamp to ensure good contact between the glass slide and the stamp during deposition of PEI. After patterning, the Wilco dishes were assembled according to the specification by the manufacturer.

Microorganisms and growth conditions

The two bacterial species *Pseudomonas putida* KT2440 and *Synechocystis sp.* PCC 6803 were used in addition to the algae Chlamydomonas *reinhardtii* CC-4532. The microorganisms where cultured under the following conditions: *P.putida* KT2440 (TOL plasmid cured derivative [44]) was grown in LB medium (10 g L^{-1} tryptone; 5 g L^{-1} yeast extract; 5 g L^{-1} NaCl) supplemented with 50 µg mL^{-1} kanamycin at 30°C over-night in shake flasks. Two different strains carrying different plasmids, pSB-B1b or a derivative of pSB-M1g, pHH100-GFP,[57] were used to express the green florescent protein variant mut3 (GFP). The pSB-B1b and pHH100-GFP plasmids express GFP from the AraC/P_{BAD} or XylS/P_m positive regulator/promoter systems, respectively. GFP expression by the AraC/P_{BAD} system is induced by L-arabinose, whereas methylbenzoic (MB) or m-Toluic acid induces the XylS/P_m system. Both plasmids are based on a mini-RK2 replicon with a kanamycin gene rendering bacteria carrying the plasmids resistant to the antibiotic

kanamycin. Both plasmids were transferred into *P. putida* KT2440 by electroporation.[58] *Synechocystis sp.* PCC 6803 cells were grown in 200 mL of BG 11 media[59] with 5 mM glucose at 30°C under continuous illumination (20 μE.m^2 s^{-1}) for 72 hours before encapsulation. The alga *Chlamydomonas reinhardtii* CC-4532 was grown in TAP medium[60] at 18°C under continuous illumination (20 μE.m^2 s^{-1}) for 72 hours before encapsulation.

Immobilization of microorganisms on microarrays

A small sample volume (~100 μL) of dispersed bacteria or algae in the culture medium (see above) was placed on the PEI microarray and incubated for 10 min (*P. putida*) or 30 min (*Synechosystis* and *Chlamydomonas*). Unattached microorganisms were removed from the microarrays by flushing with appropriate growth medium for the microorganism in question before covering the surfaces with medium.

Synthesis of biocompatible fluorinated surfactant

A biocompatible fluorinated surfactant containing two oligomeric perfluorinated polyethers (Krytox® FSH 157, DuPont) attached to polyethelyne glycol (Jeffamine® ED-2003, Huntsman) was synthesized as described by Holze and coworkers.[61] The surfactant was used to stabilize the emulsion droplets of the alginate microbeads prepared in the microfluidic device as well as for the stabilization of double emulsions.

Encapsulation of microorganisms in alginate microbeads with droplet microfluidics

The microfluidic device used for the encapsulation of cells in alginate hydrogels (Fig. 3a) exploit hydrodynamic flow focusing for emulsification of alginate pregel solutions and has previously been described by our group.[37] The outer phase consists of hydrofluoroether (HFE7500, 3M®) with 1% (wt/vol) of the fluorinated surfactant and two aqueous inner phases: (1) precursor 0.6% (wt/vol) alginate solution with 84 mM CaEDTA and 40 mM MOPS at pH 6.7 and (2) precursor 0.6% (wt/vol) alginate solution with 84 mM ZnEDDA and 40 mM MOPS at pH 6.7. We applied a recently reported method for introducing Ca^{2+} for controlling kinetic of ionotropic gelation of alginate.[36] The approach exploits an ion exchange mechanism yielding a biocompatible and device friendly gelation process of alginate and under physiological pH.[37] The concentration of the microorganism and the flow rates of the microorganism dispersion and alginate solutions were controlled to obtain microbeads with only a few bacteria in each gel bead. Following the microfluidic assisted droplet generation and on-chip gelation, the cells immobilized in the alginate microbeads were collected in a cell flask containing appropriate medium for the encapsulated cells under constant stirring. We used 10% (v/v) LB in TAP, BG 11 medium and TAP medium for the *P.putida*, *Synechosystis* and *Chlamydomonas* respectively. The collected microbeads were subsequently washed to remove the fluorinated surfactant by adding 20% (v/v) perfluorooctanol (PFO) to the collection tube, centrifuging at 2000 rpm for 2 min and discarding the supernatant (oil, surfactant and PFO). The microbeads were finally re-suspended in appropriate cell medium. A Leica SP5 confocal microscope was used to investigate the microorganisms that were encapsulated in microbeads. Image in Fig. 3a was captured with a Fastcam SA3 high speed camera (Photron). Image in Fig. 3b was captured with the Leica SP5.

Micro-pipette aspiration and re-suspension of selected encapsulated bacteria

A mixture of two cultures of *P.putida*, 20% containing the pSB-B1 plasmind and 80% carrying the p100-GFP plasmid, were encapsulated in alginate microbeads. The microbeads were stored in 10% (v/v) LB medium in TAP containing 50 mM arabinose. The arabinose induces GFP production only in the bacteria carrying the pSB-B1 plasmid. The microbeads were subsequently anchored on PEI microarrays as described above, covered in medium, and imaged using a confocal microscope (Leica SP5). The encapsulated *P.putida* containing the pSB-B1 plasmid and thus synthesizing GFP in presence of arabinose was easily detected with the confocal microscope and collected using a glass capillary (D_o: 100-120 μm D_i: 30-50 μm) mounted on a micromanipulator and connected to a syringe (BD plastic) with plastic tubing. A single microbead was ejected into a disposable tube (BD Falcon®) with LB-medium containing 50 μg mL^{-1} kanamycin and incubated over night at 30°C under constant agitation. After 24 hours incubation the cells originally transferred to the tube by micropipette assisted transfer of a particular alginate micro bead had given rise to a high number of bacterial cells. Arabinose was added to the suspension to a final concentration of 50 mM. The culture was subsequently incubated (1 hour, 30°C) before the bacteria where imaged using the confocal microscope.

Anchoring of cell-loaded alginate hydrogels onto micro-patterned PEI microarray

The washed cell loaded microbeads were immobilized on the PEI microarrays. This was carried out by adding 0.5-1 mL of medium containing approximately 20 μL of cell-loaded alginate hydrogels per 1 mL of medium onto the PEI patterned glass surfaces and allowed the beads to sediment for 15 minutes. Unanchored alginate microbeads were removed by rinsing with medium using a disposable pipette. Care was taken to avoid drying of the microarray while rinsing. After rinsing, the dish was filled with the medium appropriate for the microorganism in question.

Encapsulation of *P. putida* in (W/O/W) double emulsions and injection into 3D PDMS microarray chamber device

The microfluidic device used for the encapsulation of *P. putida* in double emulsions (Fig. 7a) exploit hydrodynamic flow focusing and a 3D step for emulsification and has previously been described by others.[50] A *P. putida*-containing inner aqueous phase with 0.15% (wt/vol) alginate dissolved from 3% (wt/vol) with LB-medium was injected with a flow rate of 50 μL

hr^{-1}. The same fluorinated oil and fluorosurfactant used for the production of alginate microbeads was used, here as the middle phase, and injected with a flow rate of 200 µL hr^{-1}. The outer aqueous phase consisted of 10% (wt/vol) PVA dissolved in LB-medium and 100 g L^{-1} sucrose and was injected with a flow rate of 800 µL hr^{-1}. The double emulsions were collected in 1 mL Eppendorf® tubes. Images in Fig. 7a were captured with the high speed camera. Image in Fig. 7c was captured with a quantitative phase contrast microscope (Zeiss axio observer Z1).

P. putida-laden double emulsions were injected into the 3D PDMS microarray chamber device using a plastic syringe (BD plastic) with plastic tubing while monitoring using an inverted optical microscope (Olympus IX70). The double emulsions were left for 2 min to sediment and flushed out with a solution containing 10% (wt/vol) PVA dissolved in LB-medium, 100 g L^{-1} sucrose and 0.5 mM m-Toluic acid. Images in ESI Fig. 1 were captured with the high speed camera.

Conclusions

The development of techniques to study bacterial populations at the single cell level provides a means to enhance our understanding of heterogeneity in bacterial populations, including its underlying causes. We propose the encapsulation of microorganisms in micron sized alginate hydrogels and double emulsions as an easy and versatile method for imaged based analysis of a high number of single cells in ordered arrays. Such microarray presentation opens for efficient microscopic inspection of high numbers of single cells, including also longitudinal studies. The approach does not involve direct contact between the encapsulated cells and the surface of the arrays, and the successful presentation of the microorganisms are therefore independent of the specific adhesion capacities of the microorganism to the surface. In this paper subsequent isolation of identified single alginate microbeads from the array and regrowth of the cellular content of the isolated bead was also demonstrated. This illustrates that sensitive single cell analysis, including extension to PCR-based protocols for measuring large panels of mRNA from single cells, can be applied on cells identified in heterogeneous populations through microscopy of arrays. In addition to the fundamental interest in understanding heterogeneity in bacterial populations, such studies are also likely to have clinical relevance related to the topics such as chronic infections and antibiotic resistance in microorganisms. The array concept presented here is not limited to the studied microorganisms and may be utilized to encapsulate mammalian cells as well.[36, 37] This opens for additional applications such as cell-based assays for drug screening[62] and for the study of the interplay between biochemical and biophysical cues that control adipogenic differentiation of hMSCs,[63] for example.

Acknowledgements

The Research Council of Norway is acknowledged for the support to the Norwegian Micro and Nano-Fabrication Facility, NorFab (197411/V30). GE is financially supported by the Swiss National Science Foundation (SNSF, No. 200021_155997). We are grateful to Rahmi Lale, Gunvor Røkke and Jacob Joseph Lamb for supplying the microorganisms used in this work. Berit Løkensgard Strand is thanked for the generous donation of alginate samples used in this work. The authors would like to thank David C. Bassett for scientific discussions related to this work.

References

1. M. B. Elowitz, A. J. Levine, E. D. Siggia and P. S. Swain, *Science*, 2002, **297**, 1183-1186.
2. I. Golding, J. Paulsson, S. M. Zawilski and E. C. Cox, *Cell*, 2005, **123**, 1025-1036.
3. A. Schmid, H. Kortmann, P. S. Dittrich and L. M. Blank, *Current Opinion in Biotechnology*, 2010, **21**, 12-20.
4. A. Gruenberger, W. Wiechert and D. Kohlheyer, *Current Opinion in Biotechnology*, 2014, **29**, 15-23.
5. V. Lecault, A. K. White, A. Singhal and C. L. Hansen, *Current Opinion in Chemical Biology*, 2012, **16**, 381-390.
6. B. Okumus, S. Yildiz and E. Toprak, *Current Opinion in Biotechnology*, 2014, **25**, 30-38.
7. A. Cerf, J.-C. Cau, C. Vieu and E. Dague, *Langmuir*, 2009, **25**, 5731-5736.
8. N. B. Arnfinnsdottir, V. Ottesen, R. Lale and M. Sletmoen, *Plos One*, 2015, **10**.
9. N. Arnfinnsdottir, A. Bjørkøy, R. Lale and M. Sletmoen, *RSC Advances*, 2016, **6**, 36198-36206.
10. A. Pannier, U. Soltmann, B. Soltmann, R. Altenburger and M. Schmitt-Jansen, *Journal of Materials Chemistry B*, 2014, **2**, 7896-7909.
11. R. Iino, Y. Matsumoto, K. Nishino, A. Yamaguchi and H. Noji, *Frontiers in Microbiology*, 2013, **4**.
12. A. I. Hochbaum and J. Aizenberg, *Nano Letters*, 2010, **10**, 3717-3721.
13. S. Rozhok, Z. Fan, D. Nyamjav, C. Liu, C. A. Mirkin and R. C. Holz, *Langmuir*, 2006, **22**, 11251-11254.
14. A. Cerf, J.-C. Cau and C. Vieu, *Colloids and Surfaces B-Biointerfaces*, 2008, **65**, 285-291.
15. L. Xu, L. Robert, O. Qi, F. Taddei, Y. Chen, A. B. Lindner and D. Baigl, *Nano Letters*, 2007, **7**, 2068-2072.
16. D. B. Weibel, A. Lee, M. Mayer, S. F. Brady, D. Bruzewicz, J. Yang, W. R. DiLuzio, J. Clardy and G. M. Whitesides, *Langmuir*, 2005, **21**, 6436-6442.
17. M. M. Mossoba, S. F. Al-Khaldi, J. Kirkwood, F. S. Fry, J. Sedman and A. A. Ismail, *Vibrational Spectroscopy*, 2005, **38**, 229-235.
18. J.-H. Kim, D.-Y. Lee, J. Hwang and H.-I. Jung, *Microfluidics and Nanofluidics*, 2009, **7**, 829-839.
19. J. Kim, Y.-H. Shin, S.-H. Yun, D.-S. Choi, J.-H. Nam, S. R. Kim, S.-K. Moon, B. H. Chung, J.-H. Lee, J.-H. Kim, K.-Y. Kim, K.-M. Kim and J.-H. Lim, *Journal of the American Chemical Society*, 2012, **134**, 16500-16503.
20. I. Wong, X. Ding, C. Wu and C.-M. Ho, *Rsc Advances*, 2012, **2**, 7673-7676.
21. P. Panda, S. Ali, E. Lo, B. G. Chung, T. A. Hatton, A. Khademhosseini and P. S. Doyle, *Lab on a Chip*, 2008, **8**, 1056-1061.

22. A. Kumachev, J. Greener, E. Tumarkin, E. Eiser, P. W. Zandstra and E. Kumacheva, *Biomaterials*, 2011, **32**, 1477-1483.
23. W.-H. Tan and S. Takeuchi, *Advanced Materials*, 2007, **19**, 2696-2701.
24. J. Wan, *Polymers*, 2012, **4**, 1084-1108.
25. P. de Vos, M. Bučko, P. Gemeiner, M. Navrátil, J. Švitel, M. Faas, B. L. Strand, G. Skjak-Braek, Y. A. Morch, A. Vikartovská, I. Lacík, G. Kolláriková, G. Orive, D. Poncelet, J. L. Pedraz and M. B. Ansorge-Schumacher, *Biomaterials*, 2009, **30**, 2559-2570.
26. S. Utech, R. Prodanovic, A. S. Mao, R. Ostafe, D. J. Mooney and D. A. Weitz, *Advanced Healthcare Materials*, 2015, **4**, 1628-1633.
27. Y.-H. Lin, Y.-W. Yang, Y.-D. Chen, S.-S. Wang, Y.-H. Chang and M.-H. Wu, *Lab on a Chip*, 2012, **12**, 1164-1173.
28. L. Yu, M. C. W. Chen and K. C. Cheung, *Lab on a Chip*, 2010, **10**, 2424-2432.
29. P. S. Stewart and M. J. Franklin, *Nature Reviews Microbiology*, 2008, **6**, 199-210.
30. Y. Zhang, Y.-P. Ho, Y.-L. Chiu, H. F. Chan, B. Chlebina, T. Schuhmann, L. You and K. W. Leong, *Biomaterials*, 2013, **34**, 4564-4572.
31. H. F. Chan, Y. Zhang, Y.-P. Ho, Y.-L. Chiu, Y. Jung and K. W. Leong, *Scientific Reports*, 2013, **3**.
32. H. C. Neu, *Science*, 1992, **257**, 1064-1073.
33. T. U. Berendonk, C. M. Manaia, C. Merlin, D. Fatta-Kassinos, E. Cytryn, F. Walsh, H. Bürgmann, H. Sørum, M. Norström, M.-N. Pons, N. Kreuzinger, P. Huovinen, S. Stefani, T. Schwartz, V. Kisand, F. Baquero and J. L. Martinez, *Nature Reviews Microbiology*, 2015, **13**, 310-317.
34. C. Brunot, L. Ponsonnet, C. Lagneau, P. Farge, C. Picart and B. Grosgogeat, *Biomaterials*, 2007, **28**, 632-640.
35. A. Akinc, M. Thomas, A. M. Klibanov and R. Langer, *J. Gene Med.*, 2005, **7**, 657-663.
36. D. C. Bassett, A. G. Håti, T. B. Melø, B. T. Stokke and P. Sikorski, *Journal of Materials Chemistry B*, 2016, **4**, 6175-6182.
37. A. G. Håti, D. C. Bassett, J. M. Ribe, P. Sikorski, D. A. Weitz and B. T. Stokke, *Lab on a Chip*, 2016, **16**, 3718-3727.
38. A. R. Abate, C.-H. Chen, J. J. Agresti and D. A. Weitz, *Lab on a Chip*, 2009, **9**, 2628-2631.
39. D. Matulis, I. Rouzina and V. A. Bloomfield, *Journal of Molecular Biology*, 2000, **296**, 1053-1063.
40. J. Fu and J. B. Schlenoff, *Journal of the American Chemical Society*, 2016, **138**, 980-990.
41. V. G. Bruce, *The Journal of Protozoology*, 1970, **17**, 328-334.
42. J. J. Lamb, J. J. Eaton-Rye and M. F. Hohmann-Marriott, *Curr Microbiol*, 2013, **67**, 123-129.
43. M. Fernández, S. Conde, J. de la Torre, C. Molina-Santiago, J.-L. Ramos and E. Duque, *Antimicrob Agents Chemother*, 2012, **56**, 1001-1009.
44. M. I. Ramos-Gonzalez, M. J. Campos and J. L. Ramos, *Journal of Bacteriology*, 2005, **187**, 4033-4041.
45. B. Amsden, *Macromolecules*, 1998, **31**, 8382-8395.
46. N. Q. Balaban, J. Merrin, R. Chait, L. Kowalik and S. Leibler, *Science*, 2004, **305**, 1622-1625.
47. J. Yan, W.-A. C. Bauer, M. Fischlechner, F. Hollfelder, C. F. Kaminski and W. T. S. Huck, *Micromachines*, 2013, **4**, 402-413.
48. S. Ma, W. T. S. Huck and S. Balabani, *Lab on a Chip*, 2015, **15**, 4291-4301.
49. J. G. Riess and M. P. Krafft, *Artificial Cells Blood Substitutes and Immobilization Biotechnology*, 1997, **25**, 43-52.
50. L. R. Arriaga, E. Amstad and D. A. Weitz, *Lab on a Chip*, 2015, **15**, 3335-3340.
51. A. R. Abate, J. Thiele, M. Weinhart and D. A. Weitz, *Lab on a Chip*, 2010, **10**, 1774-1776.
52. S. C. Kim, D. J. Sukovich and A. R. Abate, *Lab on a Chip*, 2015, **15**, 3163-3169.
53. S.-H. Kim, J. W. Kim, D.-H. Kim, S.-H. Han and D. A. Weitz, *Small*, 2013, **9**, 124-131.
54. C. Martino, T. Y. Lee, S.-H. Kim and A. J. deMello, *Biomicrofluidics*, 2015, **9**.
55. T. Y. Lee, R. Praveenkumar, Y.-K. Oh, K. Lee and S.-H. Kim, *Journal of Materials Chemistry B*, 2016, **4**, 3232-3238.
56. A. Rotem, A. R. Abate, A. S. Utada, V. Van Steijn and D. A. Weitz, *Lab on a Chip*, 2012, **12**, 4263-4268.
57. S. Balzer, V. Kucharova, J. Megerle, R. Lale, T. Brautaset and S. Valla, *Microbial Cell Factories*, 2013, **12**.
58. K. H. Choi, A. Kumar and H. P. Schweizer, *Journal of Microbiological Methods*, 2006, **64**, 391-397.
59. J. J. Eaton-Rye, in *Photosynthesis Research Protocols, Second Edition*, ed. R. Carpentier, 2011, vol. 684, pp. 295-312.
60. D. S. Gorman and R. P. Levine, *Proceedings of the National Academy of Sciences of the United States of America*, 1965, **54**, 1665-1669.
61. C. Holtze, A. C. Rowat, J. J. Agresti, J. B. Hutchison, F. E. Angile, C. H. J. Schmitz, S. Koster, H. Duan, K. J. Humphry, R. A. Scanga, J. S. Johnson, D. Pisignano and D. A. Weitz, *Lab on a Chip*, 2008, **8**, 1632-1639.
62. S. Ahadian, J. Ramon-Azcon, M. Estili, R. Obregon, H. Shiku and T. Matsue, *Biosensors & Bioelectronics*, 2014, **59**, 166-173.
63. S. Gobaa, S. Hoehnel and M. P. Lutolf, *Integrative Biology*, 2015, **7**, 1135-1142.